Snapping Mechanical Metamaterials under Tension

*Ahmad Rafsanjani, Abdolhamid Akbarzadeh, and Damiano Pasini**

We present a monolithic mechanical metamaterial comprising a periodic arrangement of snapping units with tunable tensile behavior. Under tension, the metamaterial undergoes a large extension caused by sequential snap-through instabilities, and exhibits a pattern switch from an undeformed wavy-shape to a diamond configuration. By means of experiments performed on 3D printed prototypes, numerical simulations, and theoretical modeling, we demonstrate how the snapping architecture can be tuned to generate a range of nonlinear mechanical responses including monotonic, S-shaped, plateau, and non-monotonic snap-through behavior. This work contributes to the development of micro-architectured materials with programmable nonlinear mechanical responses.

Mechanical metamaterials are man-made materials, usually fashioned from repeating unit cells which are engineered to achieve extreme mechanical properties, often beyond those found in most natural materials.[1] They gain their unusual, sometimes extraordinary, mechanical properties from their underlying architecture, rather than the composition of their constituents. Metamaterials exhibit interesting mechanical properties, such as negative Poisson's ratio,[2,3] negative incremental stiffness,[4] negative compressibility,[5] and unusual dynamic behavior for wave propagation.[6] As Ron Resch (artist and applied geometrist) points out in his statement "the environment responds by collapsing quite often,"[7] instabilities can be exploited to design advanced materials with innovative properties.[8] Recently, harnessing elastic instabilities played a central role in the rational design of novel 2D[9–14] and 3D[15–17] mechanical metamaterials with either significantly enhanced mechanical properties or equipped with new functionalities, e.g., programmable shape transformations.[14] In most of the examples mentioned above, elastic instabilities are exploited to trigger a pattern switch by a broken rotational symmetry, mostly governed by Euler buckling. In these works instabilities are induced by an applied compressive load.[16] This observation naturally leads to the question of whether one can either benefit from other mechanical instability mechanisms for metamaterial design or extend current concepts to other loading conditions.

In this work, we exploit mechanical instability triggered by snap-through buckling to create a metamaterial which experiences a pseudo pattern switch in tension and exhibits a programmable mechanical response. Our design is inspired by a monolithic bistable mechanism,[18] i.e., two curved parallel beams that are centrally clamped, as schematized in **Figure 1**a. A normal force applied in the middle of the double-beam mechanism can prompt it to snap through to its second stable state (Figure 1a, dashed lines). We release clamped conditions at both ends to create a repeatable unit cell (Figure 1b), composed of two centrally connected cosine-shaped slender segments, which can be tessellated in plane to form a periodic arrangement. When pulled along its axis of symmetry (y-axis), at a critical tensile strain ε_{cr}, the lower segment snaps through, and the structure exhibits a pattern switch from a wavy-shaped structure to a diamond-like configuration (Figure 1c–e). Depending on the amplitude of the curved segments, this transition can be either smooth or discontinuous. The amplitude of the cosine-shaped curved segment can thus provide a means to tune the mechanical response of the system. We showcase the above-mentioned concept with experiments on fabricated prototypes and examine the robustness of our findings by performing finite element simulations and a theoretical analysis.

We perform experiments on 3D printed specimens (Shapeways, Inc., NY, USA) fabricated using selective laser sintering technology (EOS e-Manufacturing Solutions, Germany) from a Nylon-based rubber-like material (Young's modulus of $E \simeq 78$ MPa and Poisson's ratio $\nu \simeq 0.4$). The specimens comprised of an array of 5×5 unit cells. Three different amplitude sizes ($a/l = 0.2, 0.3, 0.4$) are considered, whereas all the other geometrical parameters are kept constant ($l = 10$ mm, $t_b = t_w =$ 1.5 mm, and $t_s = t_g = 1$ mm). The out-of-plane thickness of all samples is $b = 3$ mm. Quasi-static conditions are applied to the samples that are pulled in a uniaxial testing machine (Bose ElectroForce 3510) at a constant rate of $\dot{u}_y = 1\ \text{mm s}^{-1}$ The pulling forces and displacements are acquired, while a high-resolution digital camera facing the specimen records a video.

Figure 2a–c shows the nominal stress–strain curves (calculated as $\sigma_y = F_y/(n_x b l)$ and $\varepsilon_y = u_y/(n_y h)$ where F_y is the reaction force, u_y the displacement along y-axis, and $n_x = n_y = 5$) of the snapping mechanical metamaterials for given amplitude parameters a/l in response to a tensile load. The stress–strain curves exhibit three regions. i) A small strain regime, where the specimens respond linearly up to a critical strain $\varepsilon_{cr} = 0.2$–0.25. In this phase, the response is governed by bending-dominated deformations in the snapping segments. ii) Snapping strain regime, where a further stretching triggers elastic instabilities. The snapping segments snap through row-by-row, with relatively small changes in the tensile load, until the whole specimen is fully stretched. Here, for the smaller value of the amplitude parameter $a/l = 0.2$, the stress–strain curve reaches a plateau, whereas for larger amplitudes, i.e., $a/l = 0.3, 0.4$, the response is non-monotonic. During snapping, the slope of the stress–strain curves becomes negative, a phenomenon

Dr. A. Rafsanjani, Dr. A. Akbarzadeh, Prof. D. Pasini
Mechanical Engineering Department
McGill University
817 Sherbrooke Street West
Montreal QC H3A OC3, Canada
E-mail: damiano.pasini@mcgill.ca
Dr. A. Akbarzadeh
Bioresource Engineering Department
McGill University
21111 Lakeshore Road, Ste-Anne-de-Bellevue
Island of Montreal QC H9X 3V9, Canada

DOI: 10.1002/adma.201502809

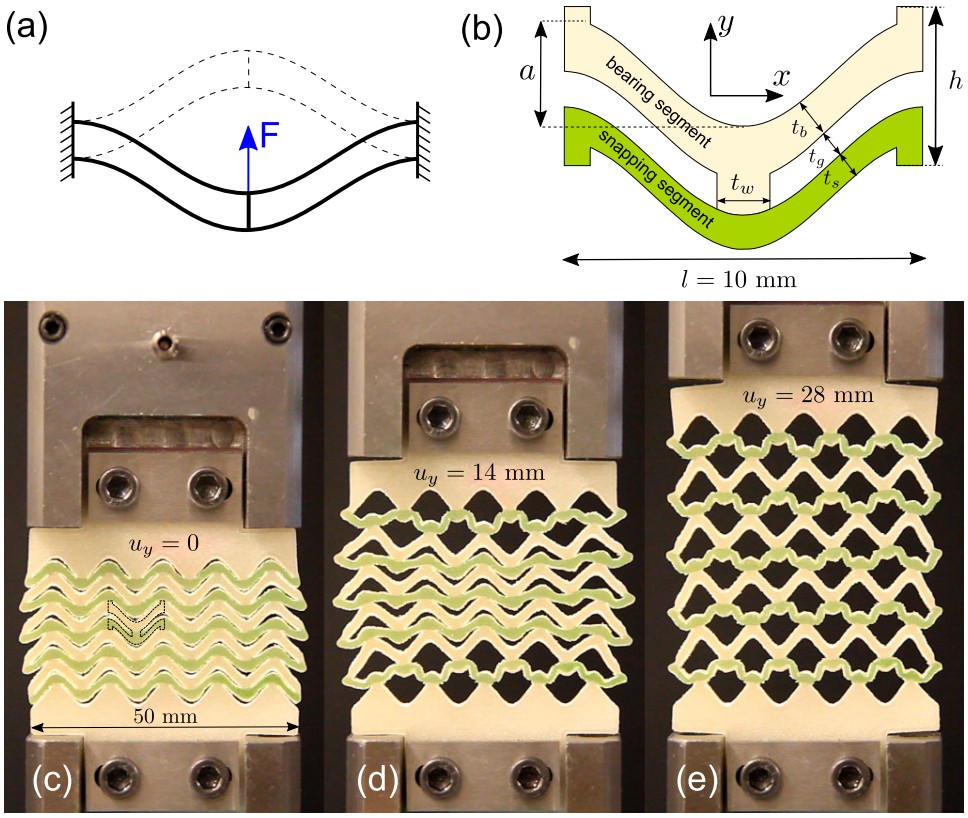

Figure 1. a) Bistable mechanism of double curved beams which can snap between two stable configurations, under a vertical force applied in the middle (adopted from Qiu et al.[18] b) Unit cell geometry of the designed metamaterial composed of load bearing and snapping segments. All samples are 3D printed from a single nylon-based rubber-like material. Afterward, the snapping segments are painted by a color marker for clarity. Under tension, the snapping segments snap through and the unit cell switches from an undeformed wavy-shape to a diamond configuration. c–e) Snapshots of the 3D printed snapping mechanical metamaterial comprised of 5×5 unit cells ($l = 10$ mm, $t_b = t_w = 1.5$ mm, and $t_s = t_g = 1$ mm) in response to tensile loading: c) undeformed state ($u_y = 0$), d) during snapping ($u_y = 14$ mm), and e) at full extension ($u_y = 28$ mm).

described by a negative incremental stiffness.[4] iii) Stiffening regime, where the cell walls orient along the loading direction, and the slope of the stress–strain curve rises again due to the transition into a fully stretching-dominated deformation state.

The response of the snapping metamaterial under uniaxial tensile loading is further investigated by performing a finite element analysis (FEA) of a full scale and a unit cell model using nonlinear FEA package ABAQUS, where all parameters match those of the experiments. The models are meshed using six-node triangular, quadratic plane stress elements (type CPS6), with mesh sensitivity analysis performed to ensure accuracy. A neo-Hookean hyperelastic material is assigned and the material parameters are adopted from the experimentally measured stress–strain curves of the solid material. A good quantitative agreement is achieved between experiments and simulations. As reflected in Figure 2a–c, all three regions observed in the experimental stress–strain curves are reproduced in the simulations, which further establishes the reliability of our computational approach. Representative examples of the simulated deformed states of each specimen are illustrated in the inset. The amplitude parameter a/l is found to affect significantly both the stress–strain relationship and the effective elastic modulus, although all the specimens are assumed to possess approximately identical porosity. Figure 2d illustrates the mechanical response of a single unit cell showing similar behavior to those observed in the experiments and full scale simulations. Here, the repeated snaps are not present, since only a single unit cell is considered. The number of rows of the unit cells along the *y*-direction governs the nonlinear mechanical response, i.e., the number of snaps, as demonstrated in the Supporting Information.[19] For $a/l = 0$, the response is monotonic and the snapping behavior vanishes.

Figure 3 shows the deformation patterns of each specimen during the three response regimes allowing a comparison with their fully stretched configurations obtained via FEA. As observed in Figure 2b,c, for large amplitudes a/l, the instabilities localize and the structure exhibits a discontinuous deformation, whereas for smaller amplitudes (Figure 2a), a smooth transition appears. A video in the Supporting Information is provided to demonstrate the deformation of the snapping metamaterials in the experiments and FEA simulations.

We systematically explore the response of unit cells under uniaxial tension to gain further insight into the mechanical responses of the metamaterial under investigation. The unit cells are stretched along the *y*-axis, whereas the deformation along the *x*-axis is restrained. To reduce the number of the parameters involved, the thickness parameters defined in Figure 1b are assumed to be identical, i.e., $t_b = t_s = t_w = t_g = 0.1l$, which implies

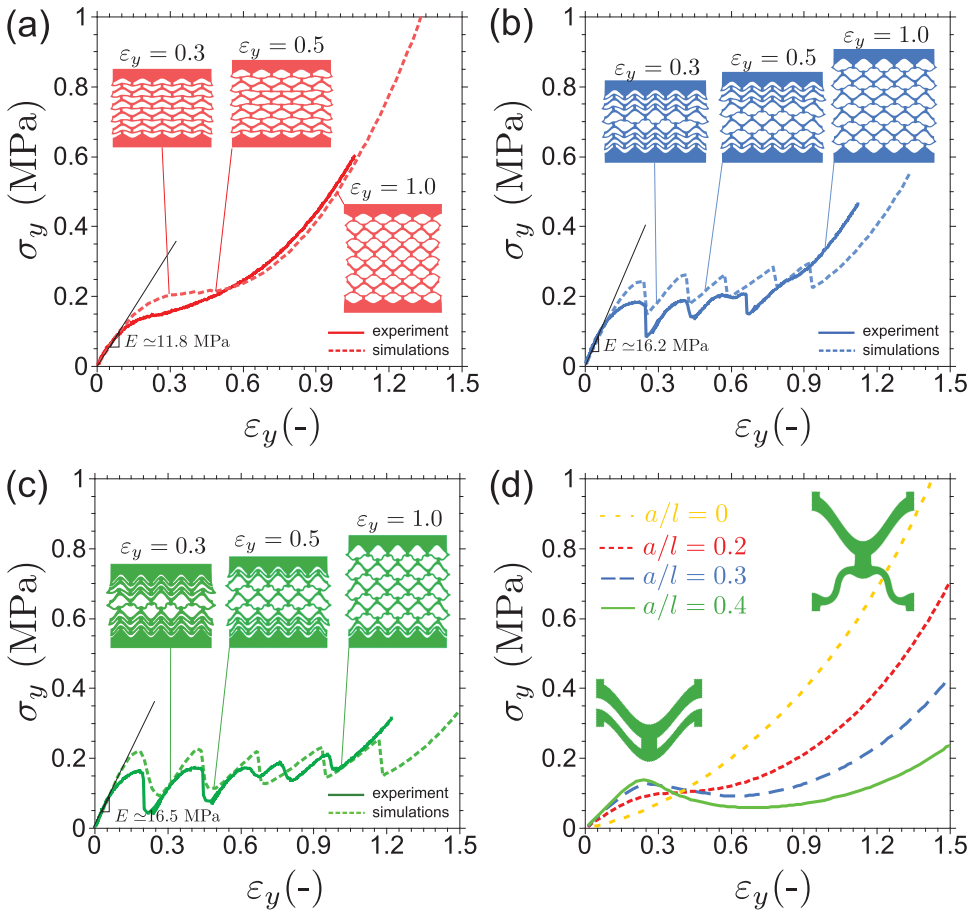

Figure 2. Nominal stress–strain responses from experiments and FEA simulations for the snapping mechanical metamaterial composed of 5 × 5 unit cells for amplitude parameters a) $a/l = 0.2$, b) $a/l = 0.3$, and c) $a/l = 0.4$. For small amplitudes of a/l, the response is smooth without snap-through instabilities, whereas for larger values of a/l, the metamaterial snaps sequentially and exhibits a discontinuous response. d) Mechanical response of a single unit cell for selected a/l parameters.

$h = 4t$. The resulting stress–strain curves from 4800 simulations in the ranges $0 \le a/l \le 0.48$ and $0.04 \le t/l \le 0.16$ are classified and a phase diagram is derived in the parameter space $(a/l, t/l)$ as shown in **Figure 4**a. The stress–strain curves fall into three categories with: i) strictly monotonic, ii) S-shaped, and iii) non-monotonic snapping responses, with representative examples for each category illustrated in the inset. Structures with small amplitudes or thick walls show a strictly monotonic stress–strain curve. The S-shaped and the snapping responses are characterized by a non-monotonic variation of the incremental stiffness. For the S-shaped responses, the incremental stiffness is positive throughout the entire range of extension, as opposed to the snapping responses where the incremental stiffness becomes negative when snapping occurs. The boundary (dashed line), separating the S-shaped curves from the snapping responses, corresponds to configurations with a plateau in their stress–strain curves, i.e., a zero incremental stiffness appears over a finite range of extension before a positive stiffness is again observed.

To better understand the nature of the mechanical behavior observed in our experiments and simulations, a soft spring model is developed. The mechanism stores the elastic strain energy via three connected elastic springs with constants k_1 and k_2 (Figure 4b). The springs are initially unstressed, and their free ends are connected to the walls by joints, which allow rotation and restrain translation. The inclined springs k_1 stand for the stiffness of the snapping segments, whereas the vertical spring k_2 represents the interaction of the snapping segments with the rest of the structure. The geometry of this mechanism is characterized by the parameters $\tilde{l}$ and $\tilde{a}$, qualitatively equivalent to the parameters l and a of the metamaterial shown in Figure 1b. The state of this mechanism is governed by the vertical position of the middle joint, where an applied vertical force F results in a vertical displacement $\tilde{u}_y$. The total potential energy of the conservative system is $W = U + \Pi$, which consists of the elastic strain energy U, stored by the springs, and the external-force potential Π. The equilibrium state of the system can be achieved from the stationary condition ($\delta W = 0$) of the total potential energy (please see the Supporting Information). In this case, the force F is obtained by

$$F = 2k_1\left(1 - \frac{\sqrt{\tilde{a}^2 + \frac{\tilde{l}^2}{4}}}{\sqrt{\left(\tilde{a} - \tilde{u}_y\right)^2 + \frac{\tilde{l}^2}{4}}}\right)\left(\tilde{u}_y - \tilde{a}\right) + k_2\tilde{u}_y \quad (1)$$

ADVANCED MATERIALS
www.advmat.de

www.MaterialsViews.com

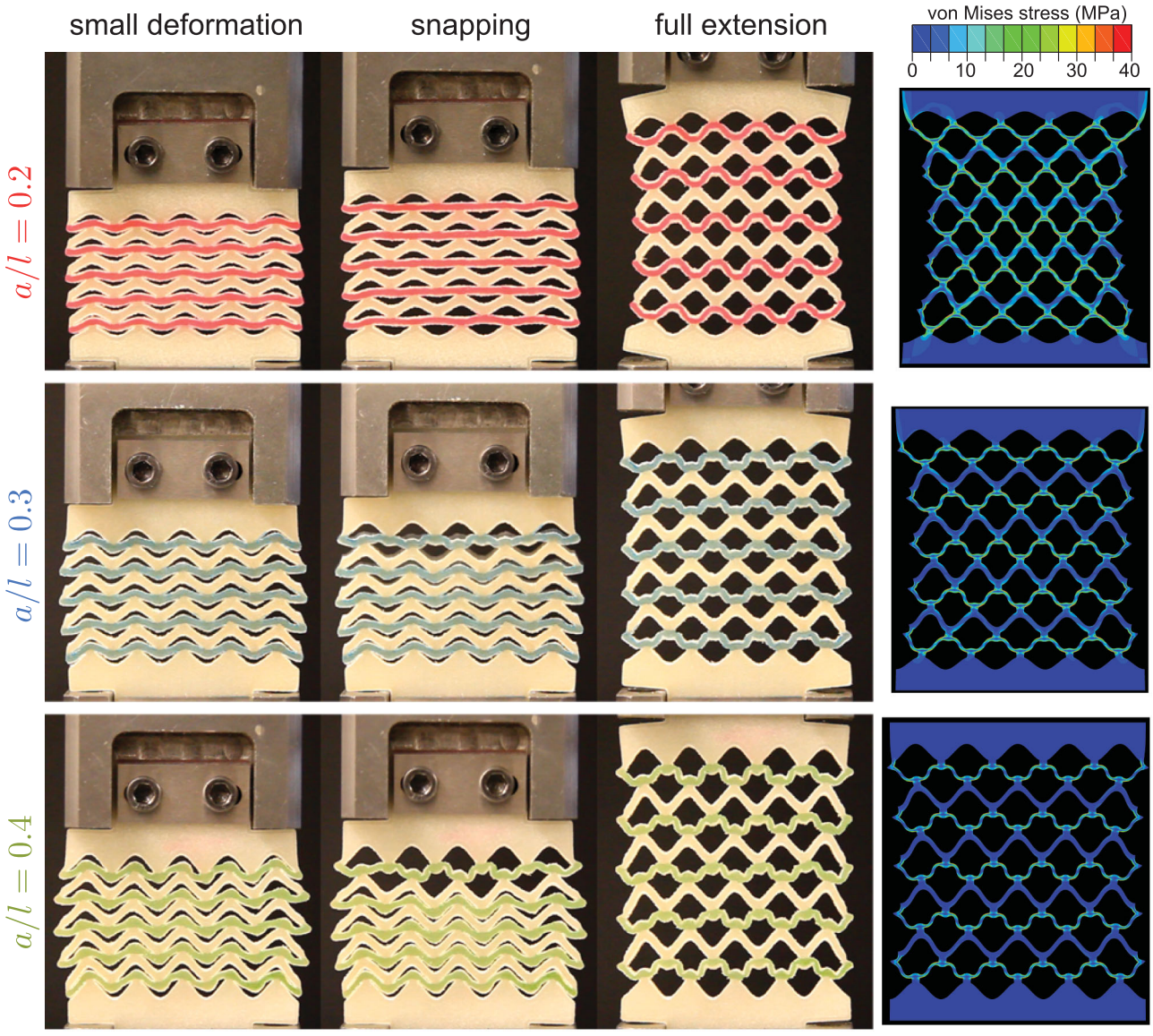

Figure 3. Snapshots of the snapping mechanical metamaterials at small deformation, onset of snapping and full extension phases for three amplitude sizes ($a/l = 0.2, 0.3, 0.4$) of the curved segments. The last column shows the FEA predictions of the deformed metamaterial at full extension and the von Mises stress distributions. All samples are 3D printed from a single nylon-based rubber-like material. To better identify where snapping occurs, a color, specific to each a/l ratio, was used to paint all the unstable segments.

Figure 4b shows the phase diagram of the soft spring system in the parameter space $\left(k_2/k_1, \tilde{a}/\tilde{l}\right)$. For $k_2/k_1 = 0$, one could expect a pure snapping behavior in the inclined springs, whereas S-shaped and plateau responses appear as k_2/k_1 increases. The plateau surface can be calculated as:

$$k_2/k_1 = 2\left(\sqrt{1+4\tilde{a}^2/\tilde{l}^2} - 1\right) \quad (2)$$

Here, the monotonic behavior occurs for $\tilde{a}/\tilde{l} = 0$, which corresponds to the response of the unit cells with very thin walls and small amplitudes of cosine-shape. The resulting phase diagram for the soft spring system is qualitatively similar to the one obtained for the unit cells. All types of observed behavior including monotonic, S-shaped, plateau, and snapping responses are captured well with this single degree of freedom, spring model.

We have studied a novel class of mechanical metamaterials whose tensile stress–strain curve can be tuned by harnessing snap-through instabilities. If pulled along the *y*-axis, it snaps sequentially from an initially wavy pattern through several metastable states till a full extension is reached. This performance makes it potentially suitable for the design of morphing, adaptive, and deployable structures. The energy dissipated via this snap-through phenomenon can be used for vibration isolation and damping applications.[20] This metamaterial can also serve as an adjustable tensile device for wave guide applications in photonic/phononic crystals.[21] The soft spring mechanism suggests that the interaction of the snapping segments with the rest

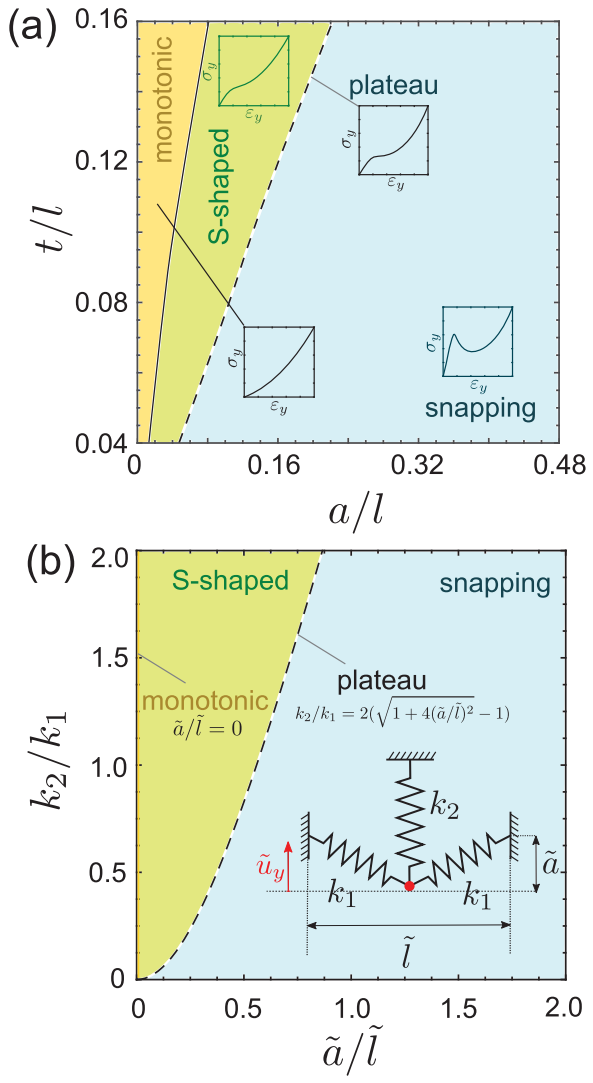

Figure 4. Phase diagrams for mechanical responses of a) unit cells under uniaxial extension in the parameter space $(a/l, t/l)$, b) for a single degree of freedom soft spring mechanism in the parameter space $(k_2/k_1, \tilde{a}/\tilde{l})$ showing monotonic, S-shaped and snapping responses and the plateau region.

of the structure can lead to mechanical responses with specific characteristics including incremental positive, zero, or negative stiffness. The experimental results and FEA predictions exhibit quantitative agreement throughout the extension range, in both the shape of the stress–strain curves and the nature of the deformation patterns. Snap-through instabilities have been employed for material design in bistable periodic structures under compressive load,[22,23] and for tuning surface topography.[24] More recently, Shan et al.[25] designed an architected material that under compression exhibits multistable energy-absorbing behavior due to snap-through instability occurring in beam-like elements. However to the best of authors' knowledge, this is the first time that snap-through buckling is embedded in mechanical metamaterials under tension and remarkably large strain is featured up to 150%. In particular, all segments in our designed metamaterial have approximately uniform thickness, a key feature that allows an even stress distribution and prevents from unpredicted failure. With several others, this work contributes to pave the way toward the study of nonlinear mechanical response of mechanical metamaterials with new functionalities.

Supporting Information

Supporting Information is available from the Wiley Online Library or from the author.

Acknowledgements

A.R. acknowledges the financial support provided by Swiss National Science Foundation (SNSF) for Early Postdoc.Mobility Fellowship under grant no. 152255. Also, A.A. acknowledges the financial support and postdoctoral fellowship by Natural Sciences and Engineering Research Council of Canada (NSERC).

Received: June 11, 2015
Revised: July 20, 2015
Published online: August 28, 2015

[1] J. H. Lee, J. P. Singer, E. L. Thomas, *Adv. Mater.* **2012**, *24*, 4782.
[2] R. Lakes, *Science* **1987**, *235*, 1038.
[3] J. N. Grima, K. E. Evans, *Mater. Sci. Lett.* **2000**, *19*, 1563.
[4] B. Moore, T. Jaglinski, T. S. Stone, R. S. Lakes, *Philos. Mag. Lett.* **2006**, *86*, 651.
[5] Z. G. Nicolaou, A. E. Motter, *Nat. Mater.* **2012**, *11*, 608.
[6] N. Nadkarni, C. Daraio, D. M. Kochmann, *Phys. Rev. E* **2014**, *90*, 023204.
[7] R. Resch, The Ron Resch Paper and Stick Film, **1992**, available from: https://vimeo.com/36122966, accessed: August 2015.
[8] N. Hu, R. Burgueño, *Smart Mater. Struct.* **2015**, *24*, 063001.
[9] T. Mullin, S. Deschanel, K. Bertoldi, M. C. Boyce, *Phys. Rev. Lett.* **2007**, *99*, 084301.
[10] K. Bertoldi, P. M. Reis, S. Willshaw, T. Mullin, *Adv. Mater.* **2010**, *22*, 361.
[11] J. T. B. Overvelde, S. Shan, K. Bertoldi, *Adv. Mater.* **2012**, *24*, 2337.
[12] J. Shim, S. Shan, A. Kosmrlj, S. H. Kang, E. R. Chen, J. C. Weaver, K. Bertoldi, *Soft Matter* **2013**, *9*, 8198.
[13] S. H. Kang, S. Shan, A. Kosmrlj, W. L. Noorduin, S. Shian, J. C. Weaver, D. R. Clarke, K. Bertoldi, *Phys. Rev. Lett.* **2014**, *12*, 098701.
[14] B. Florijn, C. Coulais, M. van Hecke, *Phys. Rev. Lett.* **2014**, *113*, 175503.
[15] J. Shim, C. Perdigou, E. R. Chen, K. Bertoldi, P. M. Reis, *Proc. Natl. Acad. Sci. USA* **2012**, *109*, 5978.
[16] S. Willshaw, T. Mullin, *Soft Matter* **2012**, *8*, 1747.
[17] S. Babaee, J. Shim, J. C. Weaver, E. R. Chen, N. Patel, K. Bertoldi, *Adv. Mater.* **2013**, *25*, 5044.
[18] J. Qiu, H. L. Lang, A. H. Slocum, *J. Microelectromech. Syst.* **2004**, *13*, 137.
[19] A. Vigliotti, V. S. Deshpande, D. Pasini, *J. Mech. Phys. Solids* **2014**, *13*, 137.
[20] R. S. Lakes, T. Lee, A. Bersie, Y. C. Wang, *Nature* **2001**, *410*, 565.
[21] K. Bertoldi, M. C. Boyce, *Phys. Rev. B* **2008**, *77*, 052105.
[22] J. Prasad, A. R. Diaz, *J. Mech. Des.* **2006**, *128*, 1298.
[23] D. M. Correa, T. D. Klatt, S. A. Cortes, M. R. Haberman, D. Kovar, C. C. Seepersad, *Rapid Prototyping J.* **2015**, *21*, 193.
[24] D. P. Holmes, A. J. Grosby, *Adv. Mater.* **2007**, *19*, 3589.
[25] S. Shan, S. H. Kang, J. R. Raney, P. Wang, L. Fang, F. Candido, J. A. Lewis, K. Bertoldi, *Adv. Mater.* **2015**, *27*, 4296.

ADVANCED MATERIALS

Supporting Information

for *Adv. Mater.*, DOI: 10.1002/adma.201502809

Snapping Mechanical Metamaterials under Tension

*Ahmad Rafsanjani, Abdolhamid Akbarzadeh, and Damiano Pasini**

WILEY-VCH

Supporting Information

Snapping Mechanical Metamaterials under Tension

Ahmad Rafsanjani[1], *Abdolhamid Akbarzadeh*[1,2] *and Damiano Pasini*[1]*

[1]*Mechanical Engineering Department, McGill University, 817 Sherbrooke Street West, Montreal, QC, H3A OC3, Canada*
[2]*Bioresource Engineering Department, McGill University, 21111 Lakeshore Road, Ste-Anne-de-Bellevue, Island of Montreal, QC, H9X 3V9, Canada*
E-mail: damiano.pasini@mcgill.ca

Effect of the number of unit cells on the snapping behavior

A parametric study is performed to investigate the role of the number of unit cells on the response of the snapping metamaterial. We consider arrays of 1×1 to 5×5 unit cells with periodic boundary conditions under uniaxial extension and present the stress-strain responses in **Figure S1**. The material properties and the geometrical parameters are isolated to the parameters used in Figure 2. For small amplitude of the parameter $a/l = 0.2$, no difference can be observed in the stress-strain curve. However, for larger amplitudes, i.e. $a/l = 0.3, 0.4$, while the unit cell responses are identical in the small strain and large strain (stiffening) regimes, they differ during the snapping phase. In this case, the number of rows governs the occurrence of the sequential snapping, which shows the role of the representative volume element size in the mechanical response of a periodic material.[19]

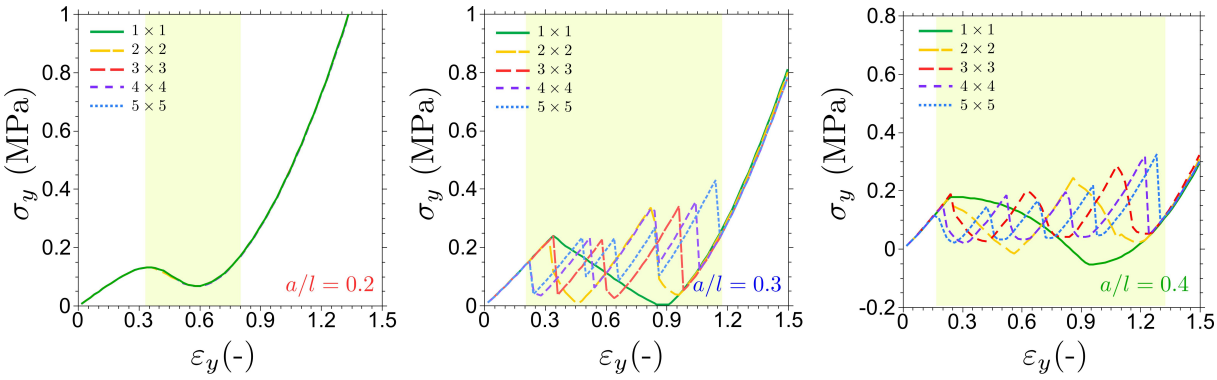

Figure S1. Nominal stress-strain curves of arrays of 1×1 to 5×5 unit cells under uniaxial extension for amplitude parameters $a/l = 0.2, 0.3, 0.4$. The highlighted regions correspond to the snapping regime.

Incremental negative stiffness vs. negative stiffness

By definition, a *negative stiffness* appears when the slope of the stress-strain curve is negative at zero force, whereas a negative slope at a non-zero load of a non-monotonic stress-strain curve represents a *negative incremental stiffness* (Moore et al., Phil. Mag. Lett. 2006, 86, 651). As shown in the phase diagram of Fig. 4a, the a/l ratio has a significant effect on the mechanical response of the metamaterial. The stress-strain curves in the snapping phase, initially exhibit a *negative incremental stiffness*. A further increase of a/l eventually results in a negative stiffness behavior, a phenomenon confirmed by the soft spring model as well. We have performed numerical simulations of a single unit cell to demonstrate the phenomenon. As shown in **Figure S2**, for $a/l = 0.1$ the stress-strain curve exhibits a positive stiffness, while negative incremental stiffness and negative stiffness responses are detected for $a/l = 0.2$ and $a/l = 0.4$, respectively. The curve of negative stiffness also presents local minima in the total energy and results in the multi-stability of the system. Therefore, the proposed unit cell could also show multi-stability. It is noteworthy mentioning that in these unit cell models, a lateral constrain is applied, a condition that facilitates a snapping response. In our metamaterial concept, however, the samples are not laterally confined. For this reason, to achieve negative incremental stiffness and negative stiffness responses, we need a relatively larger a/l ratio. For example, the sample with $a/l = 0.4$ is marginally multi-stable. We expect snapping metamaterials with $a/l > 0.4$ would exhibit a multi-stable behavior.

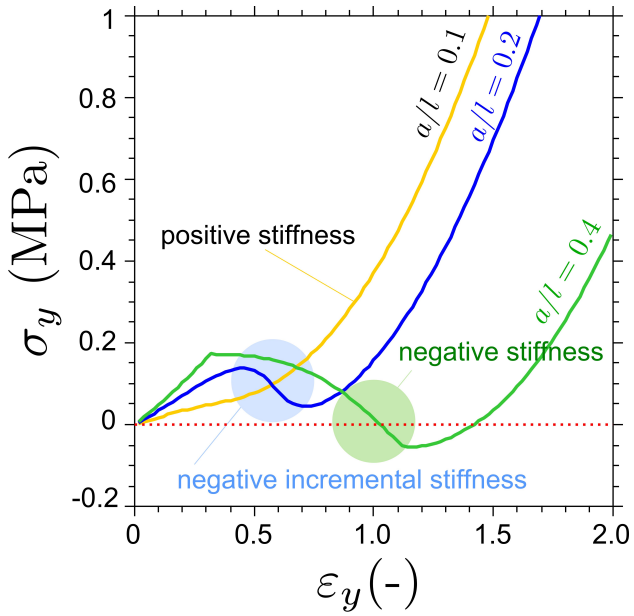

Figure S2. Nominal stress-strain curves for a unit cell ($l = 10\ mm$ and $t_b = t_w = t_s = t_g = 1\ mm$) under uniaxial extension exhibiting positive stiffness ($a/l = 0.1$), negative incremental stiffness (highlighted blue region for $a/l = 0.2$) and negative stiffness (highlighted green region for $a/l = 0.4$).

Movie description

The movie that accompanies the manuscript shows the deformation of three samples with amplitude parameters $a/l = 0.2, 0.3, 0.4$ under tensile loading and unloading with constant displacement rate $\dot{u}_y = 1\ mm/s$.

Soft spring model

As shown in the inset of Figure 4b, a soft spring model is presented to better elucidate the observed phenomena in experiments and simulations. The mechanism stores the elastic strain energy via three connected linear elastic springs. The two inclined springs (k_1) represents the snapping segments, whereas the vertical spring (k_2) stands for the interaction of the snapping segments with the rest of the metamaterial. The total potential energy of the conservative system consists of the elastic strain energy U, stored by the springs, and the external force potential Π, i.e. $W = U + \Pi$ written as:

$$W = k_1\left(\sqrt{\left(\tilde{a} - \tilde{u}_y\right)^2 + \frac{\tilde{l}^2}{4}} - \sqrt{\tilde{a}^2 + \frac{\tilde{l}^2}{4}}\right)^2 + \frac{1}{2}k_2\tilde{u}_y^2 - P\tilde{u}_y \tag{S1}$$

The equilibrium path of the system can be reached via the stationary condition of the total potential energy, i.e. $\delta W = 0$. In this case, the force (P) –displacement (u_y) relation is obtained by:

$$P = 2k_1\left(1 - \frac{\sqrt{\tilde{a}^2 + \frac{\tilde{l}^2}{4}}}{\sqrt{\left(\tilde{a} - \tilde{u}_y\right)^2 + \frac{\tilde{l}^2}{4}}}\right)\left(\tilde{u}_y - \tilde{a}\right) + k_2\tilde{u}_y \tag{S2}$$

This equation provides the response of the soft spring model in terms of the stiffness constants and geometrical features. Several force-displacement (stress-strain) scenarios, presented in the phase diagram of the Figure 4, can be distinguished via the first and second derivatives of the force with respect to the displacement. In particular, the plateau surface, in Figure 4b, corresponds to the responses that exhibit a stationary point of inflection at $\tilde{u}_y = \tilde{a}$ and for which $P' = P'' = 0$, leading to:

$$\frac{k_2}{k_1} = 2\left(\sqrt{1 + 4\left(\frac{\tilde{a}}{\tilde{l}}\right)^2} - 1\right) \tag{S3}$$

To better refine the soft spring model, a multi-degree of freedom spring system could be used.